

# Heat recovery performance of an integrated CO<sub>2</sub> commercial refrigeration system with dedicated mechanical subcooler

**Emanuele SICCO, Gabriele TOFFOLETTI, Paola D'AGARO,  
Giovanni CORTELLA**

DPIA, University of Udine, Udine, Italy, sicco.emanuele@spes.uniud.it

## ABSTRACT

CO<sub>2</sub> as a refrigerant can meet the strictest requirements in terms of safety and global warming. All-in-one plants, supplying refrigeration, heating, and air conditioning simultaneously with carbon dioxide as a working fluid, are becoming more and more common. However, in mild and hot climates CO<sub>2</sub> refrigeration plants need to implement strategies to provide an acceptable energy efficiency. Among the several possible solutions, dedicated mechanical subcooling is one of the most promising technologies. Nevertheless, the on-field monitoring of real plants which deploy these strategies is still scarce. The aim of this work is to present the results of monitoring a commercial refrigeration plant that uses CO<sub>2</sub> as a refrigerant, evaluating its heat recovery ability, and developing and validating a numerical model to predict the performance of the plant at various control logics and configurations.

Keywords: Refrigeration, Carbon Dioxide, Energy Efficiency, Monitoring, Subcooler

## 1 INTRODUCTION

CO<sub>2</sub> as a refrigerant is becoming more and more widespread in the last years in commercial refrigeration systems. This is a consequence of the most recent regulations aiming at reducing their direct greenhouse effect due to unwanted gas emissions. However, the goal of decreasing the global CO<sub>2</sub> emissions is only reached if energy use is decreased over the lifespan of the system. CO<sub>2</sub> is known to show poor performance when used in refrigeration applications at mild-warm climates, where the outdoor temperature prevents from performing subcritical operation. On the contrary, CO<sub>2</sub> is also known for the smooth temperature profile and high heat capacity during gas cooling at transcritical operation, which allows an effective heat recovery (D'Agaro et al., 2018). For this reason, one of the most widespread solutions to improve energy exploitation in commercial refrigeration systems is to use CO<sub>2</sub> in a plant for the refrigeration duty, while simultaneously supplying with the same unit the cooling power for air conditioning and/or performing heat recovery for heating purposes of the selling area, offices, and warehouse (D'Agaro et al., 2019, Giunta and Sawalha, 2021, Tsimpoukis et al., 2021, Toffoletti et al., 2024). Therefore, CO<sub>2</sub> refrigeration plants are profitably integrated with HVAC and hot water production plants, up to the all-in-one systems providing all the thermal loads of a commercial building with a high energy efficiency, as demonstrated by Karampour et al., 2017, and allowing the best match with the electrical power supply in a Demand Side Management view (Coccia, et al., 2019).

One widespread way to improve the performance of a CO<sub>2</sub> refrigerating plant is the use of a Dedicated Mechanical Subcooler (DMS), a refrigerating unit devoted to cooling CO<sub>2</sub> downstream the condenser/gas cooler. As shown by D'Agaro et al. (2021) and Llopis et al. (2016), it is a viable solution to improve the energy efficiency of a commercial refrigeration plant, and further improvements can be achieved when control rules of the system are modified appropriately (Cortella et al., 2021). As demonstrated by Illán-Gómez et al. (2023); the use of a DMS can be a useful strategy to increase the energy efficiency of heat pumps as well.

In this paper we describe a possible use of the DMS as a heat pump at winter conditions, to improve the heat recovery capabilities of an all-in-one commercial refrigeration system, aiming to provide cooling capacity for the refrigeration load and air conditioning, as well as heat for the space heating and hot water production if needed.

A real plant in a supermarket is monitored in base case operating conditions, then a model is developed to predict the performance of the whole system in heat recovery operation, with two different control logics on a traditional configuration, and with the DMS used as a heat pump.

## 2 SYSTEM DESCRIPTION

The scheme of the monitored system, which is located in Northern Italy, is depicted in Figure 1. It is a CO<sub>2</sub> booster system, that provides 89.3 kW at “medium temperature” (-8 °C) and 5.2 kW at “low temperature” (-33 °C), at nominal conditions. The evaporation pressure set of the medium temperature evaporators is 27.5 bar, while the low temperature one is 12.5 bar. The parallel compressor rack or the flash-gas valve elaborate the flash-gas generated during the first expansion process, carried out by the back-pressure valve, to maintain the liquid receiver pressure constant. Both the medium pressure rack and the parallel compressors rack are composed by two Dorin CD2400H, one working at fixed speed and one variable frequency driven-powered compressor. The low-pressure rack is composed by one fixed speed Dorin CD360M compressor.

The system is also able to face the whole space heating and air conditioning loads. Space heating is obtained by a brazed plate heat recovery heat exchanger (HRHE) located at the discharge of the medium temperature and parallel compressors, which releases heat to the heating system, through hot water and several fan coils. When space heating is required, the three-way valve located upstream the HRHE directs CO<sub>2</sub> flow through the CO<sub>2</sub>-water heat exchanger HRHE, and the refrigerant is cooled down before it enters the gas cooler. Another three-way valve is located downstream the HRHE to partially bypass the gas cooler and increase the refrigerant temperature at the inlet of the back-pressure valve. This is made to increase the amount of heat which can be recovered by increasing the fluid quality at the inlet of the liquid receiver, thus reducing the efficiency of the refrigeration system. In fact, when heat recovery is required, flash gas is not sent to the parallel compressors (which anyway are rarely switched on during the winter operation also when heat recovery is not required, due to the too low amount of flash gas generated at low gas cooler outlet temperature), but it flows through the flash gas valve, where is expanded in order to be elaborated by the medium pressure compressors instead of the parallel compressors, leading to a higher compressors discharge temperature and enthalpy, to increase the amount of heat which can be recovered by the HRHE. The system includes also an auxiliary evaporator placed outdoors at the same evaporating pressure of the medium temperature evaporators, to further increase the mass flow rate elaborated by the medium temperature compressors and consequently the heat which can be recovered by the HRHE.

The air conditioning load is satisfied by a finned pipe heat exchanger located inside the liquid receiver, where some of the liquid is isobarically evaporated to cool down the water-glycol mixture for the air conditioning system.

A Dedicated Mechanical Subcooler (DMS), with a cooling capacity of 4.47 kW at design conditions (evaporating temperature -10°C, condensing temperature 50°C) is located downstream the gas cooler, to further cool down the refrigerant flow by a brazed plate heat exchanger. It is important to note that the DMS works with an evaporation pressure higher than that at design conditions, so with a higher refrigerant density at the compressor inlet, and with a small pressure lift, so its cooling effect is much larger than that at design conditions. The plant is fully instrumented by a data acquisition system with a time step of 10 minutes composed by temperature (Carel NTC060 sensors), pressure (Carel SPKT sensors), and compressor status transducers, while the electrical energy consumption is measured by a wattmeter and water mass flow rate is an output of the electronic control of variable speed water pumps.

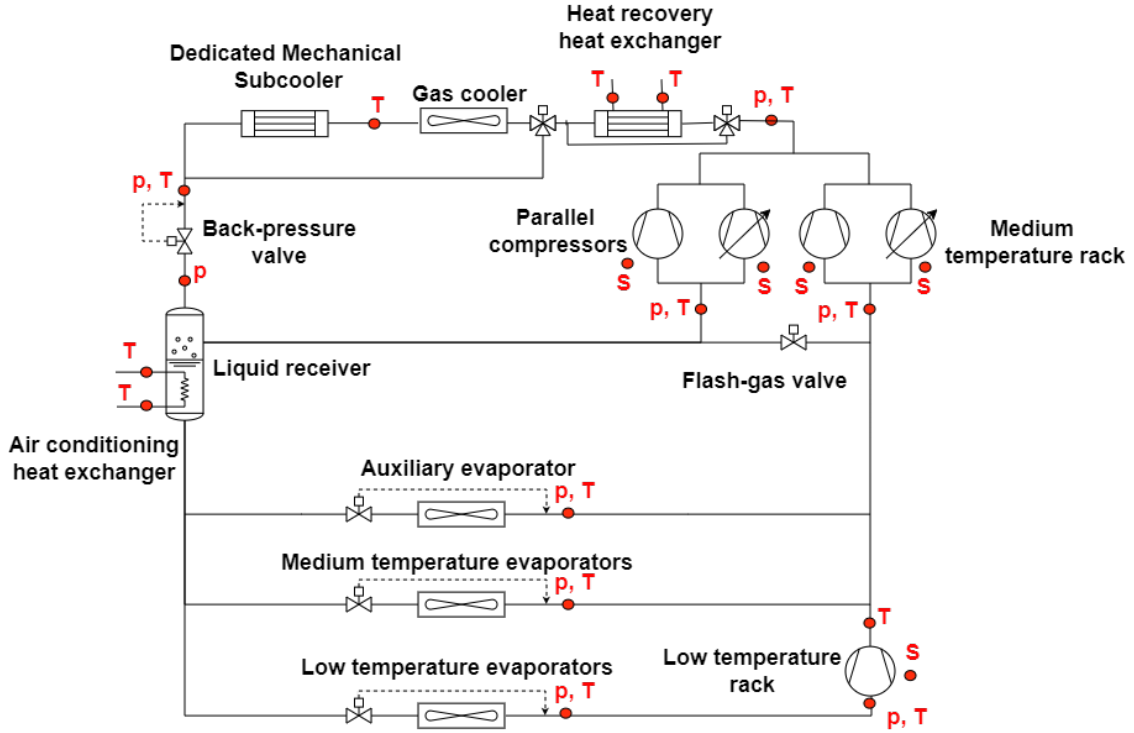


Figure 1: Sketch of the monitored plant. The positions of transducers are represented by the red dots. T: temperature transducer; p: pressure transducer; S: status of compressors transducer

### 3 MODEL DEVELOPMENT

#### 3.1 Data elaboration

The data acquired by the acquisition system have been elaborated using Matlab® software (Mathworks, 2022) with Refprop v10.0 (Lemmon et al.) to estimate the properties of refrigerants. The compressor behaviour has been modelled using the coefficients given by the manufacturer following the Standard EN12900 (EN12900:2013) for calculating the mass flow rate elaborated and the electrical power consumption. Some correction factors have been considered to take care of the difference between the test conditions defined by the norm and the actual working conditions. Both the mass flow rate and the power consumption have been corrected to consider the effect of a different actual superheating than the one used to define the coefficients (10K), since it involves changes in the density at suction side of the compressor and in the isentropic enthalpy difference from suction to discharge side of the compressor. Also, for variable speed compressors, the reductions in the global and volumetric efficiencies due to different speed have been taken into account by two correction factors depending on the frequency of compressor motor electrical power supply compared to the nominal one (50 Hz). The equations used to calculate the compressor mass flow rate  $\dot{m}_{MT}$  and absorbed electrical power  $P_{MT}$  at actual operating conditions are given in Eq. (1) and Eq. (2):

$$\dot{m}_{MT} = \dot{m}_{MT,50Hz,10K} * \frac{\rho_{actual}}{\rho_{10K}} * \left( \frac{f_{fixed}}{50} + \frac{f_{variable}}{50} * \eta_v \text{ correction} \right) \quad \text{Eq. (1)}$$

$$P_{MT} = P_{MT,50Hz,10K} * \frac{\rho_{actual}}{\rho_{10K}} * \frac{\Delta h_{is,actual}}{\Delta h_{is,10K}} * \left( \frac{f_{fixed}}{50} + \frac{f_{variable}}{50} * \frac{\eta_v \text{ correction}}{\eta_g \text{ correction}} \right) \quad \text{Eq. (2)}$$

where  $\dot{m}_{MT,50Hz,10K}$  and  $P_{MT,50Hz,10K}$  are the quantities calculated for 10K superheating and 50Hz,  $\rho_{10K}$  and  $\Delta h_{is,10K}$  are the suction density and the isentropic enthalpy difference with 10K superheating,  $\rho_{actual}$  and  $\Delta h_{is,actual}$  are the same quantities calculated with the actual superheating,  $f_{fixed}$  and  $f_{variable}$  are the actual frequencies of the compressors measured by the status of compressor transducers and  $\eta_v \text{ correction}$  and  $\eta_g \text{ correction}$  are the volumetric and global efficiency correction factors, extrapolated as a function of

the difference between the actual frequency and the nominal one. The correction factors have been defined referring to the variations of the compressor efficiency due to the variation of the compressor rotational speed described in Azzolin et al. (2021). Mass flow rate and electrical power absorbed by parallel and low temperature compressors are calculated using equations similar to Eqs. (1) and (2). For the low temperature compressors, only one fixed speed compressor is used, so the second term in brackets is null. The flash-gas generated at the liquid receiver by the first expansion process is calculated as:

$$\dot{m}_{flash-gas} = x_{in,ric} * (\dot{m}_{MT} + \dot{m}_{par}) \quad \text{Eq. (3)}$$

where  $x_{in,ric}$  is the vapour quality at the inlet of the liquid receiver, estimated using the temperature and pressure measurements upstream the back-pressure valve and the liquid receiver pressure measurement,  $\dot{m}_{MT}$  is the mass flow rate elaborated by the medium temperature compressors, calculated as in Eq. 1 and  $\dot{m}_{par}$  is the mass flow rate elaborated by the parallel compressors rack. When the heating system requires heat, the parallel compressors are switched off, to allow flash-gas to be processed by the medium temperature compressors, in order to increase the amount of heat which can be released at the HRHE, and the temperature of the CO<sub>2</sub> flow at its inlet. The refrigerating load of medium temperature evaporators in the real plant has been estimated by calculating the mass flow rate elaborated by the various compressor racks and the enthalpy difference, as shown in Eq. (4).

$$Q_{MT} = \dot{m}_{ev,MT} * (h_{in,ev} - h_{out,ev}) \quad \text{Eq. (4)}$$

where  $h_{in,ev}$  and  $h_{out,ev}$  are the enthalpy values at the inlet and outlet of the medium temperature evaporators, calculated by knowing the liquid receiver pressure and so the enthalpy of saturated liquid, the evaporating pressure and the useful superheat regulated by the expansion valves, while  $\dot{m}_{ev,MT}$  is the CO<sub>2</sub> mass flow rate at the medium temperature evaporators calculated as shown in Eq. (5).

$$\dot{m}_{ev,MT} = \dot{m}_{MT} - \dot{m}_{LT} - \dot{m}_{flash-gas} \quad \text{Eq. (5)}$$

where  $\dot{m}_{MT}$  is the mass flow rate elaborated by the medium temperature compressors (Eq. 1),  $\dot{m}_{LT}$  is the mass flow rate elaborated by the low temperature compressors and the flash-gas mass flow rate is calculated as shown in Eq. 3, or null if the parallel compressors are switched on, since the flash-gas valve is closed. Also, the heating load required by the heating system is calculated, thanks to the temperature sensors at the inlet and outlet of the on the water side of HRHE, and the mass flow rate at the water pump, as shown in Eq. (6).

$$Q_{hr} = \dot{m}_{hw} * c_{p,water} * (T_{w,out} - T_{w,in}) \quad \text{Eq. (6)}$$

$\dot{m}_{hw}$  is the water mass flow rate, estimated by the water pump control unit, and dependent on the number of fan coils in operation,  $c_{p,water}$  is the specific heat of the water, and  $T_{w,out}$  and  $T_{w,in}$  are the temperature values of water at the inlet and outlet of the heat recovery heat exchanger.

### 3.2 Model description

A quasi-steady-state thermodynamic model, with no involvement of time differential equations, with a time step of 10 minutes, has been developed, in order to simulate different control rules or configurations of the plant. All the aforementioned equations used for data elaboration have been implemented also in the model. The compressors status and frequency and the heat recovery control logic implemented in every time step are estimated, by iterative methods, to allow the plant to meet the actual measured refrigerating and heating loads, considering the power limits of the components. An empirical compression heat loss factor, dependent upon the discharge temperature estimated using the corrected polynomials, has been extrapolated from the on-field measurements, to correct the calculated discharge temperature due to heat loss in the compressor heads and in the discharge line. The HRHE has been simulated by a mean efficiency value calculated from measurements during the data acquisition period, equal to 0.80. The heat exchanged by the gas cooler has been modelled by assuming an empirical approach value function of the outdoor temperature and the status of the fans, dependent in turn on the status of the heat reclaim. The optimal gas cooler pressure, regulated by the back pressure valve, is calculated from the gas cooler outlet temperature by three different control

rules (three different sets of coefficients of the pressure control rule are used, depending from the heat rejection phase: subcritical, transcritical, or a transition between the two) when the heating system is off, while it is forced at a fixed value (91 bar) when heat recovery is activated. The superheating at the suction side of the three compressor racks has been imposed at the mean values measured during the data acquisition period, while for the values of the useful superheating at the evaporators the actual expansion valves set points have been taken. The evaporating pressures are set as in the real system. The medium temperature refrigerating load, the heating load, the water heating mass flow rate and the outdoor temperature are required as inputs by the model, while the refrigeration demand of the low temperature evaporators is considered constant and equal to the nominal one. The amount of energy used by the auxiliaries of the plant (control panel, circulating pumps, etc.) is estimated from measurements equal to the 17% of the power used by the whole system, which takes into account also the energy used by the gas cooler and auxiliary evaporator fans (in total 1.4 kW power consumption at full speed).

### 3.3 Model validation

The power consumption calculated by the model and measured by the wattmeter in every time step has been integrated to calculate the daily energy consumption. The comparison between the daily energy consumption calculated by the model and the one measured for February 2024 is shown in Figure 2.

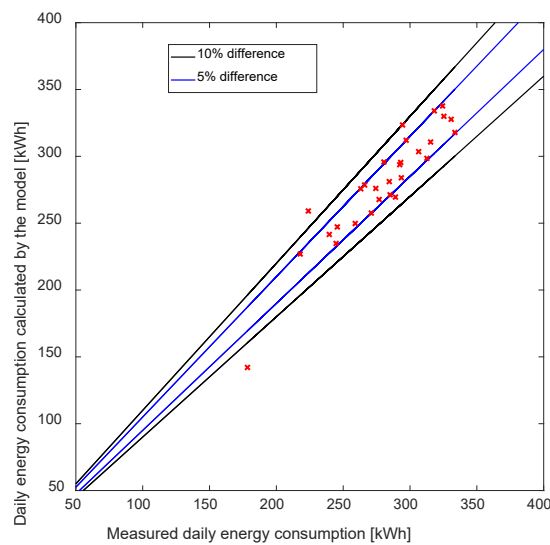


**Figure 2: Comparison between the daily electrical energy consumption calculated by the model and measured, for February 2024**

For most of the days, the estimated energy consumption differs less than 5% from the one measured, so the model can be considered reliable for the winter behaviour. Points in the (p-h) chart which represent the CO<sub>2</sub> flow conditions at the discharge side of medium temperature and parallel compressor racks (red points), at the inlet of the back-pressure valve (blue points) and at the inlet of the liquid receiver (green points) for the whole month of February 2024 are depicted in Figure 3. For the sake of clarity, the refrigerant conditions at other points of the cycle, which do not provide any additional relevant information about the plant operation, are not included in the chart. The group of gas cooler pressure conditions (blue and red points) with a pressure around 60 bar refers to the refrigerant conditions when heat recovery is not needed (subcritical conditions) and the back pressure valve maintains a gas cooler pressure function of the gas cooler outlet temperature following the normal operation rules implemented by its controller. The group of gas cooler pressure conditions (blue and red points) with a pressure around 91 bar refers to when heat recovery is activated (transcritical conditions), and the gas cooler pressure is forced to such a constant value.

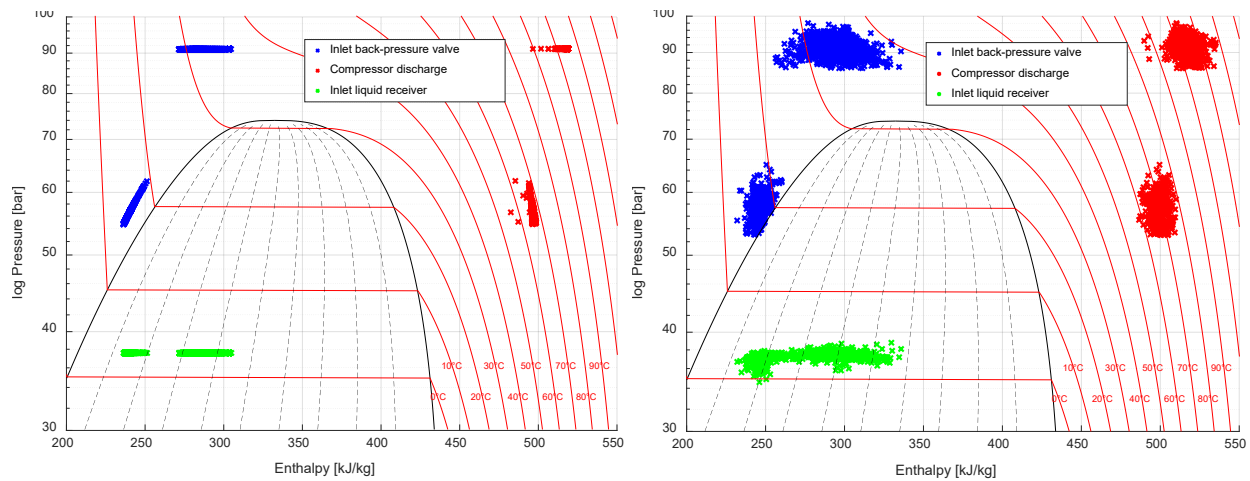


**Figure 3: Estimated (left) and measured (right) working points during February 2024**

The dispersion of measured data can be attributed to the imperfect control of the gas cooler pressure performed by the back-pressure valve, mostly due to transient operating conditions. This occurrence also influences the value of the gas cooler pressure chosen to perform the heat recovery. In fact, if a delay in the control of the valve occurs at the first expansion stage, and the gas cooler pressure decreases while the gas cooler outlet temperature remains high, this can lead to a high vapour quality of CO<sub>2</sub> at the inlet of the liquid receiver, so a too low liquid mass flow rate.

#### 4 PROPOSED CONTROL LOGICS AND PLANT MODIFICATIONS TO USE THE DMS

The model has been used for investigating two different control logics and a plant modification aimed at making the system capable of supplying the whole heat demand of the building when this is requested. The goal is to supply hot water at 42 °C, and the control logics operate so as to improve heat reclaim, often leading to worst performance from the refrigerating point of view. Of course, the refrigerating load is always guaranteed, but electrical power use may be quite different. When comparing the three cases, the heating load for the building measured in the actual application is considered.

##### 4.1 Case A

The first control logic (case A) consists of three sequential steps, activated one after the other if the actuation of the previous step doesn't guarantee enough recoverable heat by the HRHE to satisfy the heating load:

- The gas cooler pressure is raised up to 91 bar. This value is assumed to ensure that a large amount of heat recovered is available at a relatively high temperature (more than 40°C). For the same reason, the parallel compressors are forced to stay switched off to allow the medium-pressure compressor rack to handle also the flash gas generated during the first expansion stage after it has been expanded to the medium temperature evaporation pressure by the flash gas valve, leading to a higher compressors discharge temperature.
- Then gas cooler outlet temperature is increased, firstly by slowing down gas cooler fans and subsequently by modulating the gas cooler three-way bypass, which increases the temperature at the back-pressure valve inlet up to 36°C.
- Finally, the auxiliary evaporator is operated, adding up to 76 kW (the nominal power of the heat exchanger) of heat from outdoors.

##### 4.2 Case B

The second investigated logic (case B) is composed by three sequential steps, as the heating load increases:

- The gas cooler pressure is raised up to 91 bar, and the parallel compressors are forced to stay off.
- Then, the auxiliary evaporator is operated, adding up to 76 kW (the nominal power of the heat

exchanger) of heat from outdoors.

- Finally, gas cooler outlet temperature is increased through fan speed control first, and by-pass later, up to the CO<sub>2</sub> temperature value which matches the heating load.

### 4.3 Case C

The last investigated logic (case C) involves the use of a R-290 DMS, which during summer operation is air-condensed and used to decrease as much as possible the CO<sub>2</sub> temperature downstream the gas cooler. In heat recovery mode, DMS is involved in the two sequential steps, as the heating load increases:

- The gas cooler pressure is raised up to 91 bar and the parallel compressors are forced to stay off, and the three-way valve by-passes the gas cooler supplying CO<sub>2</sub> to the DMS evaporator. Simultaneously water from the HRHE is sent to the DMS condenser, a R-290-water heat exchanger, operating as an alternative to the air-cooled condenser, used during summer operation.
- The auxiliary evaporator is operated.

Doing so, all the heat rejected by the refrigerating unit can be recovered whatever the return temperature of water is. The needed modifications of the system are depicted in Figure 4.

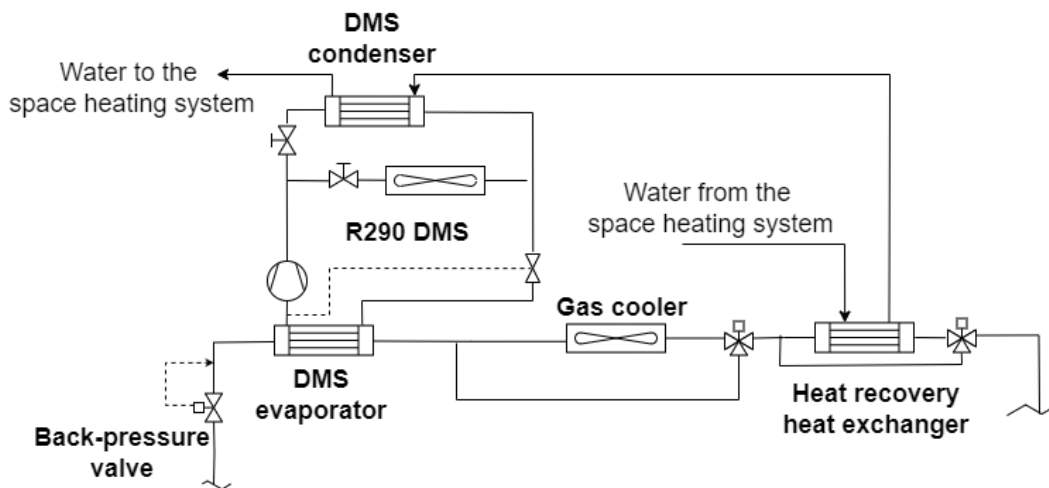


Figure 4: Case C configuration

#### 4.3.1 DMS modelling to investigate Case C

The DMS compressor is modelled by its global efficiency, calculated by a function of the evaporation temperature and the pressure ratio. This function is obtained by a regression of the global efficiency of 25 different commercially available R-290 compressors, calculated using the polynomials defined by the EN12900 Standard. The heat exchangers are supposed to be large enough to exchange all the available cooling and heating capacity, and the phase change temperature is set by an approach value. All the assumptions made for the DMS simulation are detailed in Table 1.

Table 1: Assumptions made for the DMS simulation

Superheating	10°C
Subcooling	2°C
Condenser approach	5°C
Evaporator approach	5°C
Evaporating temperature	20°C

The DMS is assumed to be regulated by the temperature of CO<sub>2</sub> upstream the back pressure valve; from an energy balance on the heat exchanger, the R-290 mass flow rate in the DMS can be calculated as in Eq. 7.

$$\dot{m}_{DMS} = \frac{\dot{m}_{CO_2} * (h_{CO_2,out rec} - h_{CO_2,out evap})}{h_{R290,out evap} - h_{R290,in evap}} \quad Eq. 7$$

where  $\dot{m}_{DMS}$  and  $\dot{m}_{CO_2,gc}$  are the DMS and CO<sub>2</sub> mass flow rates, and  $h_{CO_2,out rec}$ ,  $h_{CO_2,out evap}$ ,  $h_{R290,in evap}$  and  $h_{R290,out evap}$  are the CO<sub>2</sub> and R-290 enthalpy values at the inlet and at the outlet of the DMS evaporator, respectively. Once the R-290 mass flow rate is known, the power absorbed by the DMS compressor can be calculated as shown in Eq. (8).

$$P_{DMS} = \dot{m}_{DMS} * \frac{\Delta h_{is}}{\eta_g} \quad Eq. (8)$$

where  $P_{DMS}$  is the power absorbed by the DMS compressor,  $\Delta h_{is}$  is the isentropic enthalpy difference of the compression, and  $\eta_g$  is the global efficiency estimated by the aforementioned regression method for the selected evaporation temperature.

#### 4.4 Simulation results

The model has been used to simulate the operation of the plant during eight weeks, from the 1<sup>st</sup> of February to the 27<sup>th</sup> of March 2024, taking the real measured heating and refrigerating demands. The weekly electrical energy use in the three different cases is depicted in Figure 5. Case A results are validated as shown in Figure 2.

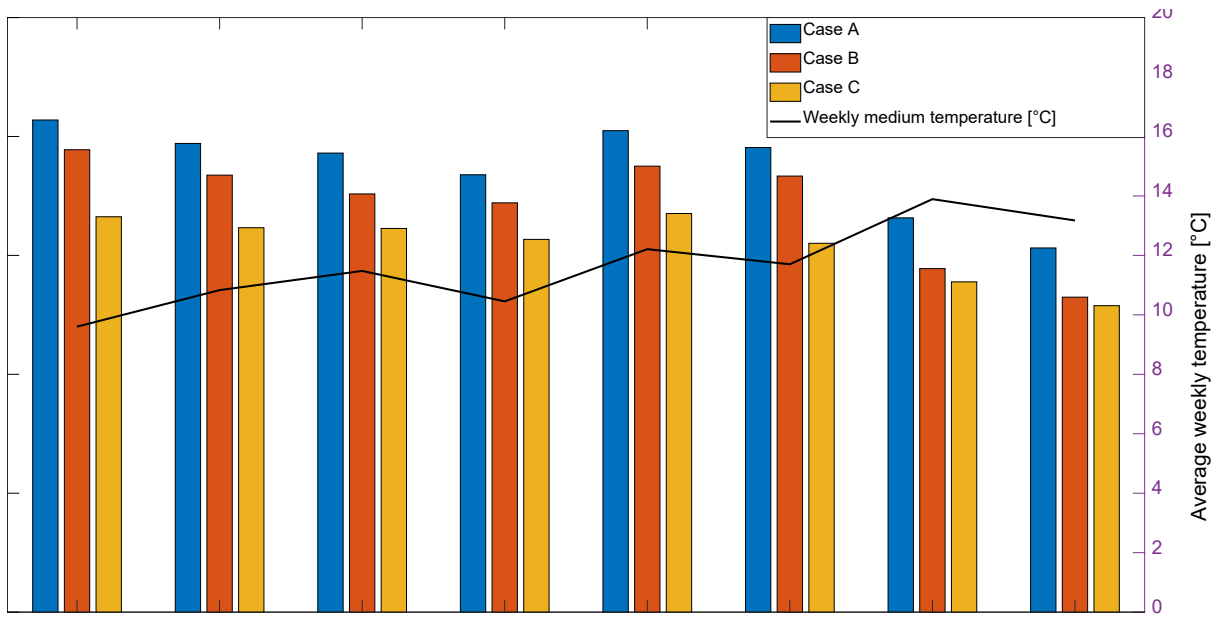
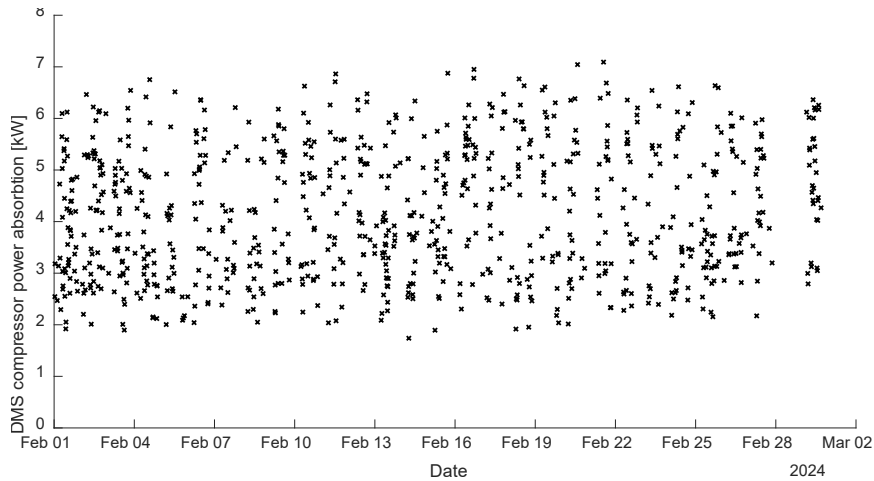


Figure 5: Week energy consumption for the three investigated cases

Case A, where the efficiency of the refrigeration plant is decreased in order to recover the correct amount of heat before operating the auxiliary evaporator, is always characterized by the lowest energy efficiency. Case B, where the auxiliary evaporator is operated as soon as the refrigerating load is not sufficient to provide enough heat reclaim, shows to allow an energy saving in all cases investigated. Case C, which requires the installation of a R-290 DMS, always requires the smallest amount of energy to meet the refrigerating and heating loads, leading to an energy saving between 14.77% and 20.61% when compared to Case A. When compared to Case B, Case C is more effective at lower outdoor temperature, while energy savings appear to reduce at mild outdoor conditions. Regarding the size of the DMS compressor, its electrical power estimated for the first 4 weeks (February 2024) with the highest heating loads is depicted in Figure 6.





**Figure 6: Power absorbed by the DMS compressor during the month of February**

The electrical power used by the R-290 DMS compressor never exceeds 7.1 kW. The size of its compressor can be considered acceptable when compared to that of the medium and parallel racks, both characterized by a nominal installed power of 32.6 kW.

## 5 CONCLUSIONS

In this work, a CO<sub>2</sub> integrated plant located in a mild-climate, able to supply both the refrigerating demand, at medium and low temperature, and the space heating and air conditioning loads, has been monitored and simulated. A thermodynamic model, refined through observations and empirical correction factors coming from the behaviour of the actual system, has been developed and validated during winter operation. Three different plant control logics have been investigated. The actual refrigerating and heating loads, derived from plant monitoring, have been implemented in the simulations. The simulation has been performed considering 8 weeks between February and March 2024, when the average weekly temperature has been between 9.6°C and 13.9°C. Different control logics have been investigated, to allow the system to supply the whole heating needs by using an auxiliary evaporator placed outdoors and/or a Dedicated Mechanical Subcooler (DMS). The most efficient sequence of operations has been identified when using the auxiliary evaporator, that is increasing the refrigeration load earlier than by-passing the gas cooler. The availability of a DMS allows its operation as a heat pump, making it possible to recover heat at a lower temperature. This solution has proven to be the most energy-efficient one, leading to a decrease in the weekly energy consumption up to 20.61% when compared to the base case. However, costs have to be investigated on an annual basis, considering the opportunity of using the DMS at high outdoor temperature.

## ACKNOWLEDGEMENTS

The research leading to these results has received funding from the MIUR of Italy within the framework of the PRIN2017 project « The energy flexibility of enhanced heat pumps for the next generation of sustainable buildings (FLEXHEAT) », grant 2017KAAECT.

Arneg SpA is gratefully acknowledged for the technical discussions and information.

## REFERENCES

- Azzolin M., Cattelan G., Dugaria S., Minetto S., Calabrese L., del Col, D. (2021). Integrated CO<sub>2</sub> systems for supermarkets: Field measurements and assessment for alternative solutions in hot climate. *Applied Thermal Engineering*, 187. <https://doi.org/10.1016/j.applthermaleng.2021.116560>
- Coccia G., Arteconi A., Polonara F., Cortella G., D'Agaro P., 2019. Demand side management analysis of a supermarket integrated HVAC, refrigeration and water loop heat pump system. *Applied Thermal*

- Engineering, (152)543-55. DOI 10.1016/j.applthermaleng.2019.02.101
- Cortella G., Coppola M.A., D'Agaro P., 2021. Sizing and control rules of dedicated mechanical subcooler in transcritical CO<sub>2</sub> booster systems for commercial refrigeration. *Applied Thermal Engineering*, (193),116953. DOI 10.1016/j.applthermaleng.2021.116953
- D'Agaro P., Cortella G., Polzot A., 2018. R744 booster integrated system for full heating supply to supermarkets. *International Journal of Refrigeration*, (96) 191-200. DOI 10.1016/j.ijrefrig.2018.09.028
- D'Agaro P., Coppola M.A., Cortella G., 2019. Field tests, model validation and performance of a CO<sub>2</sub> commercial refrigeration plant integrated with HVAC system. *International Journal of Refrigeration*, (100) 380-391. DOI 10.1016/j.ijrefrig.2019.01.030
- D'Agaro P., Coppola M.A., Cortella G., 2021. Effect of dedicated mechanical subcooler size and gas cooler pressure control on transcritical CO<sub>2</sub> booster systems. *Applied Thermal Engineering*, (182) 116145. DOI 10.1016/j.applthermaleng.2020.116145
- EN12900:2013. Refrigerant compressors - Rating conditions, tolerances and presentation of manufacturer's performance data.
- Giunta F., Sawalha S., 2021, Techno-economic analysis of heat recovery from supermarket's CO<sub>2</sub> refrigeration systems to district heating network, *Applied Thermal Engineering*, (193), 117000. DOI 10.1016/j.applthermaleng.2021.117000
- Illán-Gómez F., García-Cascales J. R., Velasco F. J. S., Otón-Martínez R. A. (2023). Numerical performance of a water source transcritical CO<sub>2</sub> heat pump with mechanical subcooling. *Applied Thermal Engineering*, 219, 119639. DOI 10.1016/j.applthermaleng.2022.119639
- Karampou M., Sawalha S. 2017, Energy efficiency evaluation of integrated CO<sub>2</sub> trans-critical system in supermarkets: A field measurements and modelling analysis. *International Journal of refrigeration*, (82), 470-486. DOI 10.1016/j.ijrefrig.2017.06.002.
- Lemmon E. W., et al., NIST Standard Reference Database 23: Reference Fluid Thermodynamic and Transport Properties-REFPROP, Version 10.0, National Institute of Standards and Technology.
- Llopis R., Nebot-Andrés L., Cabello R., Sánchez D., Catalán-Gil J., 2016. Experimental evaluation of a CO<sub>2</sub> transcritical refrigeration plant with dedicated mechanical subcooling. *International Journal of Refrigeration*, (69)361–368. DOI 10.1016/j.ijrefrig.2016.06.009
- The MathWorks, Inc. 2022. MATLAB version: 9.13.0 (R2022b).
- Toffoletti G., Cortella G., D'Agaro P., 2024, Thermodynamic and economic seasonal analysis of a transcritical CO<sub>2</sub> supermarket with HVAC supply through ice thermal energy storage (ITES). *Journal of Cleaner Production*, (434) 139832. DOI 10.1016/j.clepro.2023.139832
- Tsimpoukis D., Syngounas E., Petsanas D., Mitsopoulos G., Anagnostatos S., Bellos E., Tzivanidis C., Vrachopoulos M., 2021, Energy and environmental investigation of R744 all-in-one configurations for refrigeration and heating/air conditioning needs of a supermarket, *Journal of Cleaner Production*, (279) 123234. DOI 10.1016/j.clepro.2020.123234